Research Square

Preprints are preliminary reports that have not undergone peer review.
They should not be considered conclusive, used to inform clinical practice,
or referenced by the media as validated information.

The Evolutions in Time of Probability Density Functions of Polydispersed Fuel Spray-The Continuous Mathematical

Shlomo Hareli
Ben-Gurion University of the Negev
OPhir Nave (naveof@gmail.com)
Jerusalem College of Technology https://orcid.org/0000-0001-5499-0036
Vladimir Gol'dshtein
Ben-Gurion University of the Negev

Research article

Keywords: Poly-disperse spray, Particle-size distribution dynamics, Probability density function Dynamics, Numerical analysis, Spray combustion

Posted Date: August 10th, 2021

DOI: https://doi.org/10.21203/rs.3.rs-777585/v1

License: This work is licensed under a Creative Commons Attribution 4.0 International License.
Read Full License

The Evolutions in Time of Probability Density Functions of Polydispersed Fuel Spray-The Continuous Mathematical Model

Shlomo Hareli[a,*],

Ophir Nave[b]

Vladimir Gol'dshtein[c]

[a*] Department of Mathematics, Ben-Gurion University of the Negev,

[b] Department of Mathematics, Jerusalem College of Technology,

[c] Department of Mathematics, Ben-Gurion University of the Negev *

August 4, 2021

*$E-mail\ addresses$: harelish@post.bgu.ac.il (Sh. Hareli), Naveof@gmail.com (O. Nave), vladimir@bgu.ac.il (V. Gol'dshtein)

Abstract

The dynamics of the particle-size distribution of the polydispersed fuel spray are important for the evaluation of the combustion process. In this paper, we presented the particle-size distribution change in time which gives a new insight into the behavior of the droplets during the self-ignition process. Semenov was the first to shows that self-ignition in the homogeneous case can be qualitatively and even quantitatively described by simplified models [1]. A simplified model of the polydisperse spray is used for a study of combustion processes near the initial region. This model involves a time-dependent function of the particle-size distribution. Such simplified models are particularly helpful in understanding qualitatively the effect of various sub-processes.

Our main results show that during the self-ignition process, the droplets' radii decrease as expected, and the number of smaller droplets increases in inverse proportion to the radius. An important novel result (visualized by graphs) demonstrates that the mean radius of the droplets, at first increases for a relatively short period of time, and that is then followed by the expected decrease. It means that the maximum of the mean radius is not located at the beginning of the process as expected. We only have a heuristic explanation of this phenomenon, but an analytic study is planned for the future. Our modified algorithm is superior to the well known 'parcel' approach because it is much more compact, it permits an analytical study since the right-hand sides are smooth, and thus eliminates the need for a numerical algorithm transitioning from one parcel to another, The method explain herein can be applied to any approximation of the particle-size distribution, and it involves comparatively negligible computation time.

Keywords: Poly-disperse spray, Particle-size distribution dynamics, Probability density function Dynamics, Numerical analysis, Spray combustion

Nomenclature

A constant pre-exponential rate factor

C molar concentration ($kmolm^{-3}$)

c specific heat capacity ($Jkg^{-1}K^{-1}$))

E activation energy ($Jkmol^{-1}$)

L liquid evaporation energy (i.e., latent heat of evaporation, Enthalpy of evaporation) (Jkg^{-1})

n_{d_i} number of droplets of size i per unit volume (m^{-3})

Q combustion energy (Jkg^{-1})

B universal gas constant ($Jkmol^{-1}K^{-1}$)

R_{d_i} radius of size i drops (m)

$R_{max,0}$ maximal droplet radius at $t = 0$ (m)

T temperature (K)

t time (s)

t_{react} $A^{-1}e^{1/\beta}$ (s)

$P(\cdot)$ probability density function

$\hat{P}(\cdot)$ probability distribution function

$U(\cdot)$ Unit step function

$\Pi(\cdot)$ Rectangle function

Greek symbols and dimensionless parameters

α dimensionless volumetric phase content

ν the quantity equivalent to the volumetric phase content for the continuous model

β dimensionless reduced initial temperature (with respect to the so-called activation temperature E/B)

γ dimensionless parameter that represents the reciprocal of the final dimensionless adiabatic temperature of the thermally insulated system after the explosion has been completed

ϵ_1, ϵ_2 dimensionless parameters introduced in Eq. 2.11 and describing the interaction between gaseous and liquid phases

μ molar mass ($kgkmol^{-1}$)

λ thermal conductivity ($Wm^{-1}K^{-1}$)

ρ density (kgm^{-3})

τ dimensionless time

Ψ represents the internal characteristics of the fuel (the ratio of the specific combustion energy and the latent heat of evaporation) and defined in equation 2.11 (dimensionless)

Dimensionless variables

η dimensionless fuel concentration

θ dimensionless temperature

r dimensionless radius

Subscripts

d liquid fuel droplets

f combustible gas component of the mixture

g gas mixture

i number of droplet sizes

L liquid phase

p under constant pressure

s saturation line (surface of droplets)

0 initial state

m number of droplet sizes

Abbreviations

PDF probability density function

PSD particle-size distribution

1 Introduction

Any study of particle size distributions (PSD) dynamics can help provide insight into combustion processes. Despite the importance of this aspect of spray combustion, there is a scarcity of theoretical and numerical works on this subject which is mainly due to constraints inherent in the situation being studied (for example [2, 3, 4]). Most of the main mechanisms of such combustion processes are still unknown. But the methods and dynamics described herein add to our insight.

Recall that commonly used approximations of the initial experimental polydisperse size distributions are the following: Rosin-Rammler distribution, Nukiyama-Tanasawa distribution and Gamma distribution [5, 6]. These approximations provide comparatively accurate fittings of experimental data that allow extrapolation for values beyond the measurement scope. These approximations permit comparatively easy calculations of parameters of interest since they already built-into the computer software (e.g. MATLAB, MATHEMAICA). But to the best of our knowledge, there is not a single mathematical theory that will accurately and precisely fit experimental data. Still, in the absence of a theoretical basis, the Rosin-Rammler distribution is commonly used and allows us to describe combustion dynamics using raw experimental data.

Most attempts to theoretically describe combustion processes that accompany polydispersed sprays have resulted in complex systems of highly nonlinear partial differential equations[7]. The main difficulty is to separately describe the dynamics of individual droplets or groups of droplets that compose the fuels. Semenov pioneered the description of thermal explosion processes for gaseous fuels by simple ordinary differential equations [1]. History has shown that simplified Semenov-type models can often describe the main characters of self-ignition in the homogeneous case. But the models built on Semenov's work that focused on sprays quickly became very complex when accounting for various droplet radii [8]. The well known 'parcel' method divides droplets into separate sections, but due to computation complexity, this approach fails to estimate a realistic distribution. We did not find literature which reports any works that used more than 5-6 'parcels', we attributed this to the increased computational problems that accompany each additional parcel.

In [9] the authors proposed to use smooth probability density functions that approximate discrete droplet radii distributions instead of a separate analysis of individual droplets, the 'parcel' approximations. In this paper, polydispersity is modeled using smooth probability density functions (PDF) that correspond to the initial distribution of the size of the fuel droplets. This

approximation of a polydisperse spray is more accurate than the traditional 'parcel' approximation, and it permits an analytical treatment of the corresponding simplified model. Let us remark that any analytical treatment of the 'parcel' models is almost impossible because the right-hand sides in such models are discontinuous. This the main reason why they are infrequently used. To the best of our knowledge, a maximum of 5-6 'parcels' was used.

In [9] the probability density function approximations were compared with the 'parcel' approximations for 300 'parcel' and found more accurate. Details about this comparison can be found in [9], section 3.

Corresponding new models are low-dimensional and compact. In the case of ignition processes, such models use a probability density function (PDF). The density function is a smooth function of only one variable, the droplet's maximal or mean radius. Such models allowed us to monitor different probability density functions.

The main disadvantage of this approach was a rigid shape of probability density functions in time (the smooth probability density functions (PDF) correspond to the initial distribution of the size of the fuel droplets). This permitted us to obtain reasonable estimates of thermal explosion limits, but the more delicate properties of a spray's self-ignition are beyond the scope of this method.

In this paper, this problem is partially recovered. We propose here an equation for the evolution of probability density functions in time. We start from the initial particle-size distribution and study its dynamics. This modified method was applied to the well known Rosin-Rammler, Nukiyama-Tanasawa, and Gamma distribution approximations of experimental distributions. The main results show that during the self-ignition process, the droplets radii decrease as expected, while the number of the smaller droplet increase in inverse proportion to the radius.

An important novel result (visualized by graphs) demonstrates that the mean radius of droplets first increases for a short time, followed by the expected decrease. It means that the maximum of the mean radius is not located at the beginning of the process as expected. Our algorithm presented here is superior to the well known 'parcel' approach since our model is much more compact and the right-hand side of the equations are smooth. As result, we can use combinations of analytical and/or computational tools. This algorithm can be applied for any approximation of the particle-size distribution, and computation time is negligible.

In this paper, we mainly study the evolutions of probability density functions in time. **Remark**

We demonstrate the main observation using a simplified model. One reason for this simplification is the necessity to demonstrate a pure effect without additional complications by more detailed models. We plan to check the main results for more complicated models in the future.

2 Model Description

We first present constraints on combustion models. Then we present models that incorporate probability density functions that depend only on the maximal radius.

There are several standard assumptions that are commonly used for models describing the thermal explosion of vaporized fuel droplets. Our model is taken as adiabatic because ignition processes occur fast in comparison to heat losses by diffusion processes. Pressure variations are assumed to be negligible [1]. In addition, we assume that diffusion of the gas phase is inferior in comparison to the liquid phase, as a result, the heat transfer coefficient is determined by gas features [10]. We further assume that the liquid temperature is identical to the temperature of the saturated liquid because a quasi-steady-state approximation is reasonable for the vaporizing droplets [11]. Finally, the reaction is modeled in the simplest possible way as a first-order, highly exothermic chemical reaction. This means that the model is represented as a system of non-linear ordinary differential equations. Listed below are the assumptions that underlie the system of equations that describe the phenomena [8]:

$$\alpha_g \rho_g c_{pg} \frac{dT_g}{dt} = \alpha_g \mu_f Q_f A C_f e^{(-\frac{E}{BT_g})} - 4\pi\lambda_g (T_g - T_d) \sum_{i=1}^{m} R_{d_i} n_{d_i}, \tag{2.1}$$

$$\frac{d(R_{di}^2)}{dt} = \frac{2\lambda_g}{\rho_L L}(T_d - T_g),\ i = 1, ..., m,\ (m\ equations) \tag{2.2}$$

$$\frac{dC_f}{dt} = -AC_f e^{(-\frac{E}{BT_g})} + \frac{4\pi\lambda_g}{L\alpha_g\mu_f}(T_g - T_d) \sum_{i=1}^{m} R_{d_i} n_{d_i}. \tag{2.3}$$

The initial conditions are:

$$at\ t = 0 :\ T_g(t = 0) = T_{g0},\ R_{d_i} = R_{d_{i0}},\ \forall i : T_{d_i} = T_{g0},\ C_f = C_{f0}. \tag{2.4}$$

For the model above the droplet's radii distribution can be approximated by a smooth proba-

bility density function. The droplets radii sum is replaced by integral of the corresponding PDF [5] and [9] . A motivation for this approximation is based on a standard representation of the Riemann integral as a limit of the Riemann sum. It means that this approximation works better for a high number of parcels and can be less accurate for small numbers of parcels. Formally we can use any smooth function that satisfies the equality.

$$\int_0^\infty R_0 \hat{P}_0(R_0) dR_0 = \sum_{i=1}^{m} n_{d_i} R_{d_{i,0}}. \tag{2.5}$$

We used here the sub-index 0 for t=0. We use commonly known distributions, like Rosin-Rammler, Nukiyama-Tanasawa, and Gamma distributions as examples.

The corresponding normalized probability density function is given by the following equations:

$$P_0(R_0) = \frac{\hat{P}_0(R_0)}{\left\langle \hat{P}_0 \right\rangle}, \quad were; \quad \left\langle \hat{P}_0 \right\rangle \equiv \int_0^\infty \hat{P}_0(R_0) dR_0. \tag{2.6}$$

Note that the integration by variable R_0 is an approximation that corresponds to the summation over all the radii of droplets at the initial time. The droplet estimation by PDF is superior to the 'parcel' approach as the smooth PDF allows us to extrapolate experimental data for radii not appearing in the standard measurement. In addition, the PDF is not affected by the limitation of the parcels method which describes the droplet distribution poorly since it usually uses a comparatively small number of parcels due to calculation complexity.

Using (2.2) conditions the radius R can be expressed as follows:

$$R = \left(R_m^2 - R_{m,0}^2 + R_0^2\right)^{(1/2)}. \tag{2.7}$$

Thus R_0 can be viewed as a function of R.

$$R_0 = G\left(R\right) \equiv \left(R^2 - \left(R_m^2 - R_{m,0}^2\right)\right)^{(1/2)}. \tag{2.8}$$

We define the rectangle function:

$$\Pi_a(x) \equiv U_0(x) - U_a(x). \tag{2.9}$$

Here $U_0(x), U_a(x)$ are standard step functions

Using the last expressions we have:

$$F(R_m) \equiv \sum_{i=1}^{m} R_{d_i} n_{d_i} = \int_0^{R_{max,0}} R_0 P(R_0) dR_0 = \int_0^{\infty} G(R) P_0(G(R)) \Pi_{R_m}(R) dR \tag{2.10}$$

Here $P(R)$ is a corresponding smooth PDF function (Rosin-Rumbler, ...).

Finally, we obtain a non-dimensional model in the spirit of Semenov's theory. We will use the following parameters and non-dimensional variables:

$$\begin{gathered}
\tau = \frac{t}{t_{react}},\ t_{react} = A^{-1} e^{\left(\frac{E}{BT_{g0}}\right)},\ \beta = \frac{BT_{g0}}{E},\ \gamma = \frac{c_{pg} T_{g0} \rho_{g0}}{C_{f0} Q_f \mu_f} \beta, \\
\theta = \frac{E}{BT_{g0}} \frac{T_g - T_{g0}}{T_{g0}},\ \eta = \frac{C_f}{C_{f0}},\ r_m = \frac{R_m}{R_{m,0}},\ \Psi = \frac{Q_f}{L} \\
\epsilon_2 = \frac{Q_f C_{f0} \alpha_g \mu_f}{\rho_l \nu_0 L},\ \epsilon_1 = \frac{4\pi \lambda_{go} R_{m,0} \left\langle \hat{P}_0 \right\rangle \beta T_{g0}}{A Q_f C_{f0} \alpha_g \mu_f} e^{\left(\frac{E}{BT_{g0}}\right)},
\end{gathered} \tag{2.11}$$

The function $F(R_m)$ can be recalculated as a function of r_m:

$$\begin{gathered} G\left(R\right)=\left(R^{2}-\left(R_{m}^{2}-R_{m,0}^{2}\right)^{(1/2)}\right.= \\ R_{m,0}\left\{\left(\frac{R}{R_{m,0}}\right)^{2}-\left(\left(\frac{R_{m}}{R_{m,0}}\right)^{2}-1\right)\right\}^{1/2}= \\ R_{m,0}\left\{\left(\frac{R}{R_{m,0}}\right)^{2}-\left(r_{m}^{2}-1\right)\right\}^{1/2} \end{gathered} \tag{2.12}$$

Finally we obtain:

$$\begin{gathered} R_{m,0}\tilde{F}(r_m)\equiv F(R_m)=\int_0^\infty G(R)P_0(G(R))\Pi_{R_m}(R)dR= \\ R_{m,0}\int_0^\infty\left\{\left(\frac{R}{R_{m,0}}\right)^{2}-\left(r_{m}^{2}-1\right)\right\}^{1/2}P_0\left(R_{m,0}\left\{\left(\frac{R}{R_{m,0}}\right)^{2}-\left(r_{m}^{2}-1\right)\right\}^{1/2}\right)\Pi_{r_m\cdot R_{m,0}}(R)dR \\ \Rightarrow\tilde{F}(r_m)=\frac{1}{R_{m,0}}F(r_m,R_{m,0}). \end{gathered} \tag{2.13}$$

A new system of equations is the following:

$$\gamma\left(1+\beta\theta\right)^{-1}\frac{d\theta}{d\tau}=\eta e^{\left(\frac{\theta}{1+\beta\theta}\right)}-\epsilon_1\left(1+\beta\theta\right)^{1/2}\theta\tilde{F}(r_m), \tag{2.14}$$

$$\frac{d(r_m^2)}{d\tau}=-\frac{2}{3}\epsilon_1\epsilon_2\left(1+\beta\theta\right)^{1/2}\theta, \tag{2.15}$$

$$\frac{d\eta}{d\tau}=-\eta e^{\left(\frac{\theta}{1+\beta\theta}\right)}+\epsilon_1\Psi\left(1+\beta\theta\right)^{1/2}\theta\tilde{F}(r_m), \tag{2.16}$$

where: $\tilde{F}(r_m)$ is a function of the maximal dimensionless radius r_m given in (2.13).
The non-dimensional initial conditions are:

$$at\ \tau=0:\ \ \theta=0,\ \ r_m=1,\ \ \eta=\eta_0. \tag{2.17}$$

Technical Remark The equation 2.2 has another representation that will be useful for our study. Using $\frac{d(R_{di}^2)}{dt}=2R_{di}\frac{d(R_{di})}{dt}$ it can be rewritten as

$$\frac{d(R_{di})}{dt}=\frac{1}{R_{di}}\frac{\lambda_g}{\rho_L L}(T_d-T_g),\ \ i=1,...,m,\ \ (m\ equations) \tag{2.18}$$

Its dimensionless form is the following:

$$\frac{d(r_m)}{d\tau} = -\frac{1}{3r_m}\epsilon_1\epsilon_2 \left(1+\beta\theta\right)^{1/2}\theta. \tag{2.19}$$

The right-hand sides of 2.18 and its dimensionless version are not Lipschitz functions and have a singularity point where $R_m = 0$. Our analysis of the model does not include the values of R_m that are very close to zero. Let us also mention that for very small radii the model itself is not properly relevant [12].

3 Results and Discussion

Three widely used probability density functions for theoretical interpretations of experimentally measured droplets radii distributions are Rosin-Rammler distribution [13], Nukiyama-Tanasawa distribution [14] and the well known Gamma distribution. Their distribution parameters permit to fit most of the experimental data. Some experimental distributions and/or their approximations by known theoretical distributions that are used, normalized and, presented in the figure below (figure 3.1):

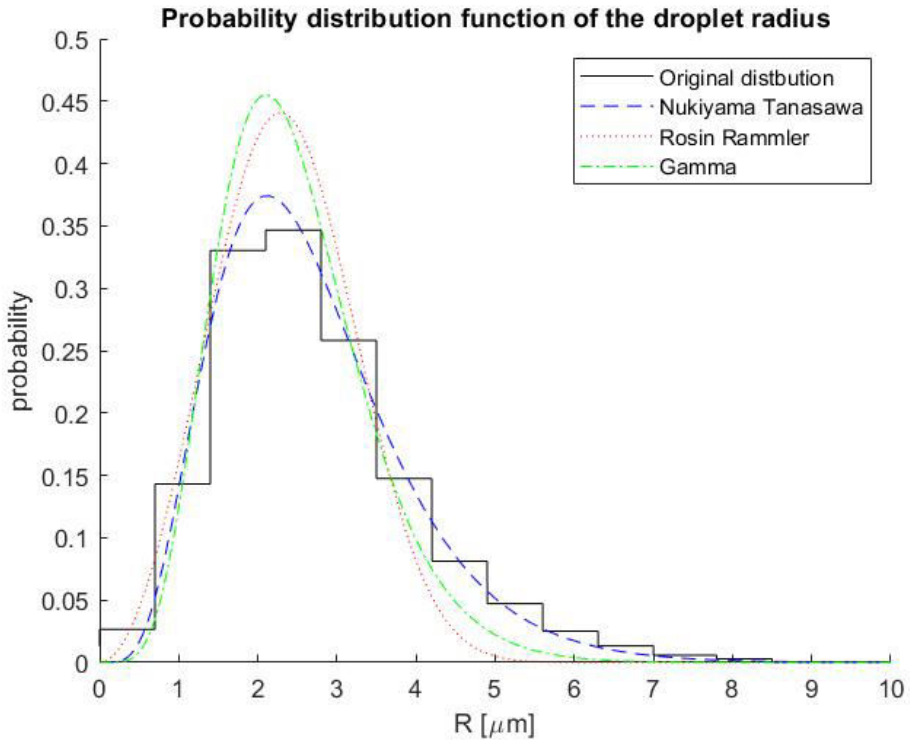

Figure 3.1: Normalized experimental probability distributions and various approximation by probability density functions (Nukiyama Tanasawa, Rosin Rammler and Gamma distributions) of the droplets radii

In the region close to $r_m = 1$ we observed an almost linear behavior of the maximal radius r_m as a function of time. It corresponds to the initial fast motion (evaporation). Close to this almost "linear" region our model is valid, thus we can study the various types of dynamic, which describes the particle-size distribution. The integrand of F represents the particle size distribution

(PSD). This conclusion immediately follows from the definition of F (2.10). On the other side, the integrand of $\tilde{F}$ is proportional to the PSD (it can be seen by equation 2.13). The dynamic of the PSD is based on the initial partial size distribution (initial measurement) and its different approximations by various commonly used probability density functions.

As we can observe (figure 3.2) the behavior of different integrands of $\tilde{F}$ is quantitatively very similar. The experimental particle size distribution is discontinuous because it is discrete and divided into several parcels, while all approximations are smooth. The integrands of F consist of $P_0(G(R))\Pi_{R_m}(R)$ that can be described with the help of probability density functions (more accurately it is proportional to the probability density functions).

With the help of the current more accurate model (comparatively with its previous version [9]) we can observe a dynamical behavior of the probability functions. Results are given below (figure 3.4).

Recall that the function F is integral that depends on r_m. In figure 3.3 you can see graphs of the integrand of F and the area under the graph is a visualization of F. The area can be also reinterpreted as a function of the droplet mean radius. As the maximum radius decreases, it will be reasonable to suppose that the mean radius will decrease as well.

Our computations demonstrate a different type of behavior of the mean radius in the initial time period. We observe an increase of the mean radius for a short period of time followed by the expected behavior (i.e., the decrease of the mean radius). Similar behavior is also observed for a different probability function (figure 3.5). This phenomenon is a stable numerical phenomenon. We have a heuristic explanation only and hopefully will be derived analytically in the future.

We can observe this numerical phenomenon of mean radius increasing for any studied probability density function. Let us observe, for example, a behavior of the integrand of the Nukiyama-Tanasawa approximation (figure 3.6) in time. For a heuristic explanation of this observation, we can analyze in more details the equation 2.18. Recall the equation:

$$\frac{d(R_{di})}{dt} = \frac{1}{R_{di}} \frac{\lambda_g}{\rho_L L}(T_d - T_g), \ i = 1, ..., m, \ (m \ equations) \tag{3.1}$$

For $T_d < T_g$ the gas temperature is superior to the temperature of the droplets, the derivative is negative. The reduction of droplet radii in time is also valid since the radius decreased in the high-temperature environment. As can be seen, the curve of any droplet density function is

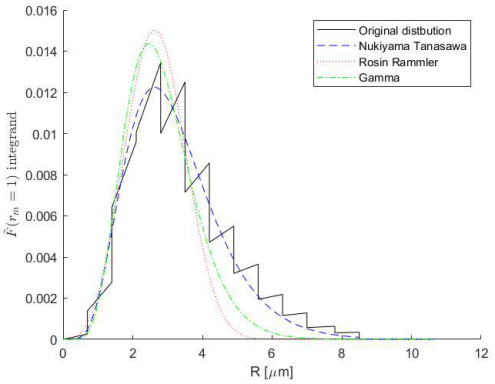

(a) The integrand of $\tilde{F}$ at $r_m = 1$

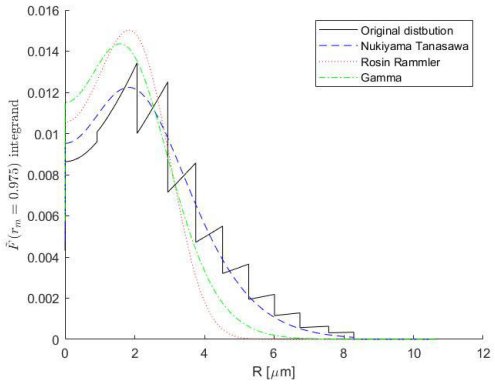

(b) The integrand of $\tilde{F}$ at $r_m = 0.975$

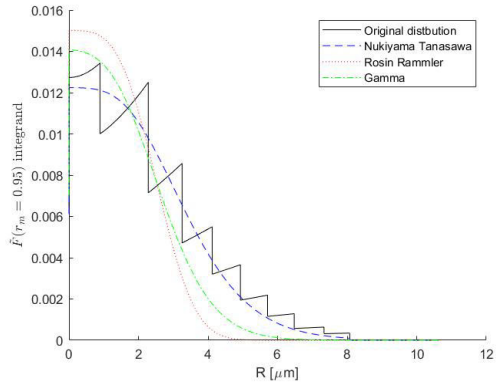

(c) The integrand of $\tilde{F}$ at $r_m = 0.95$

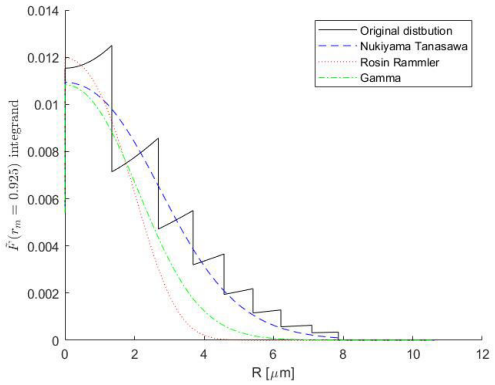

(d) The integrand of $\tilde{F}$ at $r_m = 0.925$

Figure 3.2: The integrand of $\tilde{F}$ given by equation 2.13 at region near $r_m = 1$ for experimental data and its approximations (Nukiyama Tanasawa, Rosin Rammler and Gamma distributions), at various values of r_m.

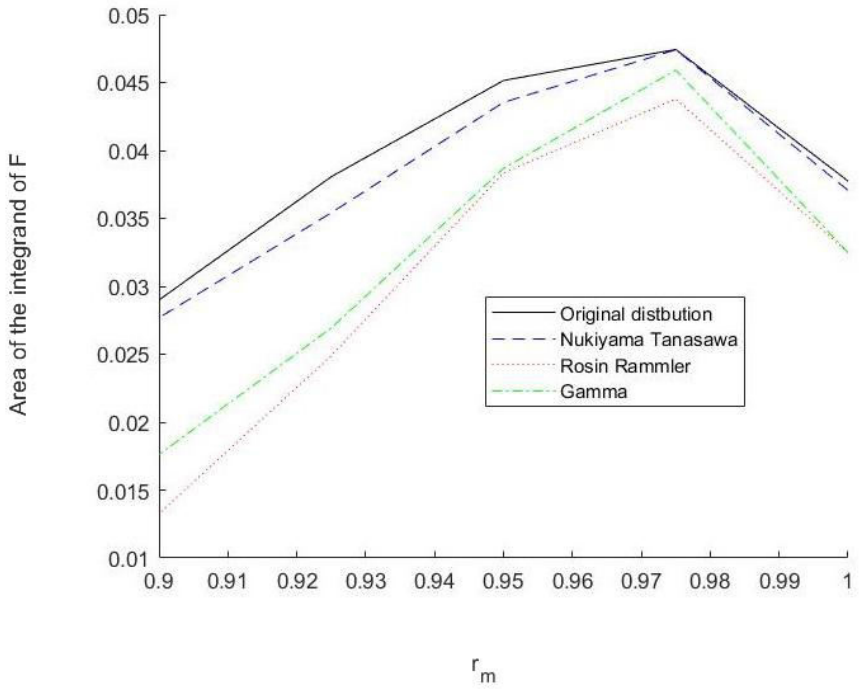

Figure 3.3: Integrand of F given by equation 2.10

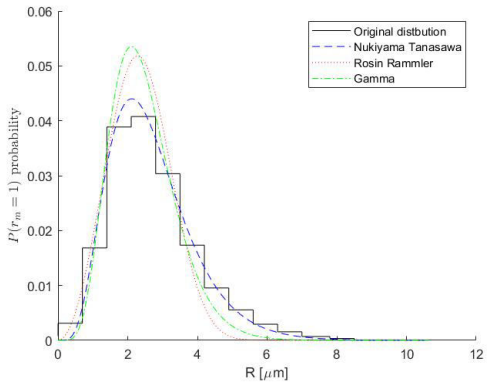

(a) Probability at $r_m = 1$

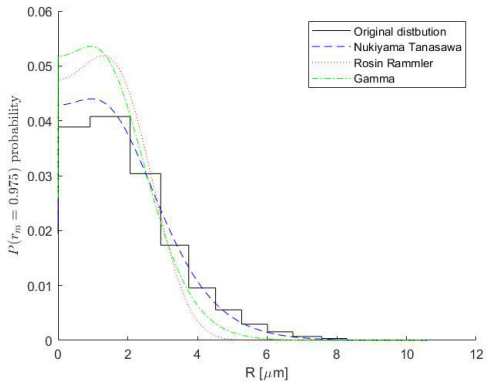

(b) Probability at $r_m = 0.975$

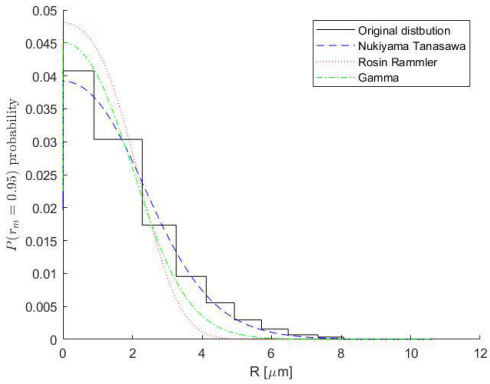

(c) Probability at $r_m = 0.95$

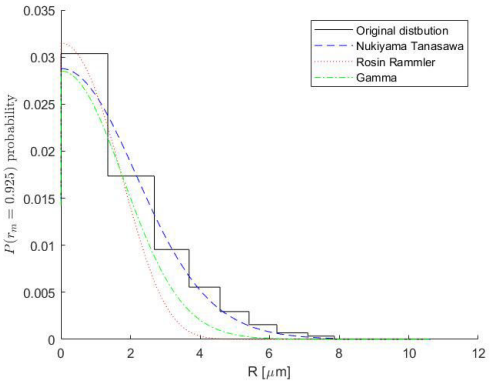

(d) Probability at $r_m = 0.925$

Figure 3.4: Nukiyama-Tanasawa, Rosin-Rammler and Gamma probability for various r_m values

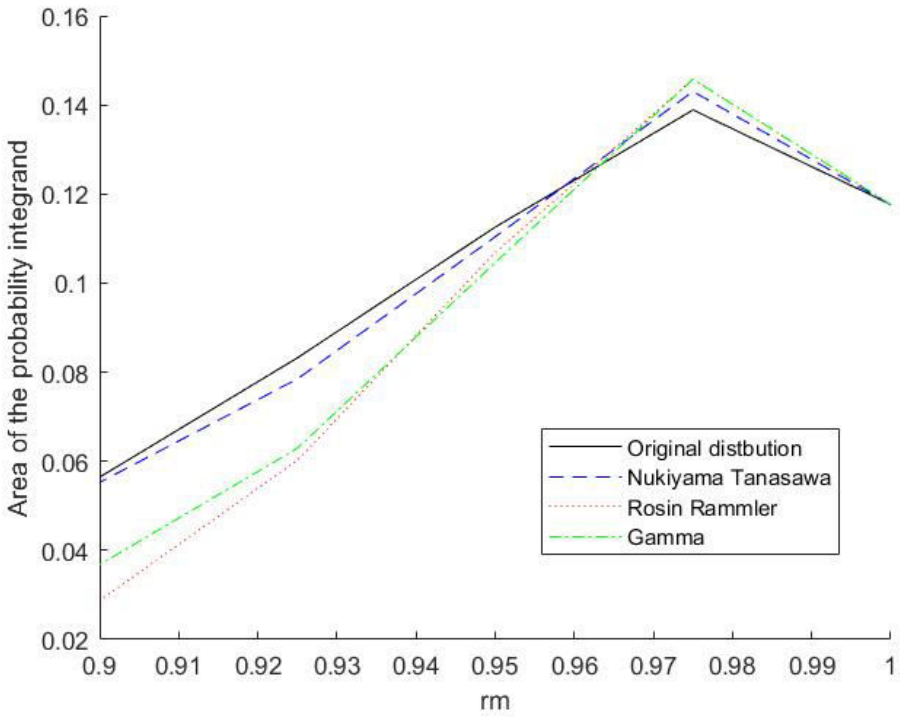

Figure 3.5: The area of the probability integrand as a function of the r_m for the various distributions (Nukiyama-Tanasawa, Rosin-Rammler and Gamma).

shifted to the right with respect to time, as expected. The shift occurs due to the reduction of the droplet size. A more important observation is the following. For any droplet, its radius reduction is proportional to the inverse of the radius. The last insight shows that droplets of a big radius will decrease in size more slowly than droplets with a smaller radius. This phenomenon is seen in the graph, where the numbers of small radius droplets rise as time increases.

A possible explanation is the following. Droplets with a higher ratio between surface and volume are more influenced by heat. From this remark, it follows that the reduction in the size of smaller droplets is faster than that for larger ones. It can be seen analytically because derivatives of droplets' radii are proportional to the inverse of their radii. Heuristically, it means that smaller droplets become less influential for the mean radius than bigger ones. Of course, this heuristic explanation is not an accurate explanation but for the moment we have not any accurate proof of the phenomena.

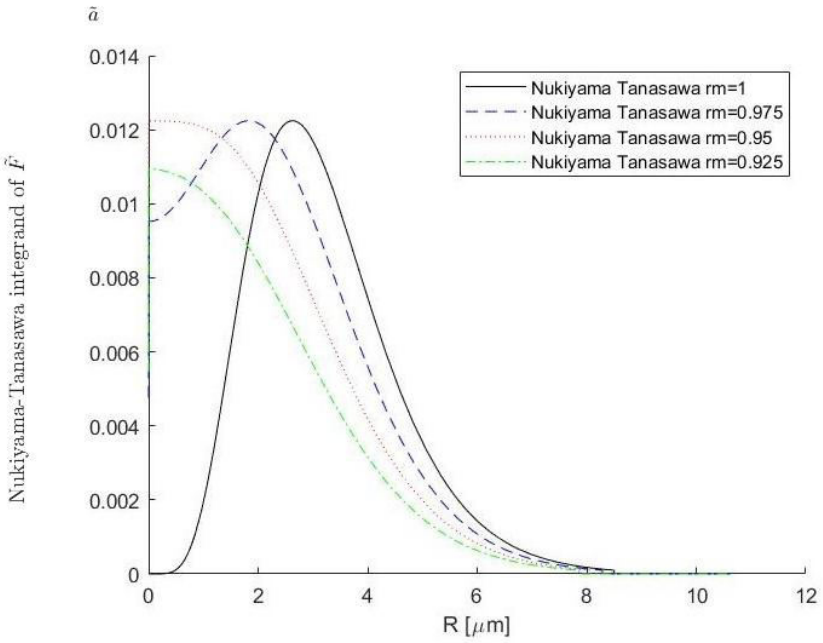

Figure 3.6: Nukiyama-Tanasawa integrand of $\tilde{F}$ given by equation 2.13 for verious values of r_m

Availability of data and materials: Not applicable

Competing interests:Not applicable

Funding: Not applicable

Authors' contributions:Not applicable

Acknowledgements:Not applicable

4 Conclusion

In this paper we essentially modified an approach proposed in our previous work [9] where we used smooth probability density functions for approximations of droplet radii distributions. This modification helps us to follow to the dynamics of the particle size distribution. Low computation time of the proposed approach provided a computational ability to accurately follow the dynamics of the experimentally measured particle-size distribution as well as its different smooth approximations. These smooth approximations allowed us to explore the behavior of the particle size distributions using a combination of analytical and computational methods. Our approach is superior to the well known 'parcel' approach due to computational problems that limited this approach to a small amount of parcels. Our results show that the mean radius of the droplets eventually decrease but surprisingly initially increase. We associate this phenomena of the increase of the mean radius to tendency of smaller droplets to evaporate at a higher rate. The ability to research the evolution in time of the complex system of droplets in the ignition process opens a window to an interesting new field in the analytical and numerical study of spray combustion.

References

[1] N. N. Semenov, "Zur theorie des verbrennugsprozesse," *Zeitschrift fur Physik*, vol. 48, pp. 571–581, 1928.

[2] S. K. Aggrawal, "A review of spray ignition phenomena: present status and future research," *Progress in Energy and Combustion Science*, vol. 24, no. 6, pp. 565–600, 1998.

[3] R. Stone, "Introduction to Internal Combustion Engines," *Macmillan, London*, 1998.

[4] E. M. Sazhin, S. S. Sazhin, M. R. Heikal, V. I. Babushok, and R. A. Johns, "A detailed modeling of the spray ignition process in diesel engines," *Combustion Science 429 and Technology*, vol. 160, no. 1, pp. 317–344, 2000.

[5] E. Babinsky and P. E. Sojka, "Modeling drop size distributions," *Progress in Energy and Combustion Science.*, vol. 28, no. 4, pp. 303–329, 2002.

[6] A. Urbán and V. Józsa, "Investigation of Fuel Atomization with Density Functions," *Periodica Polytechnica Mechanical Engineering*, vol. 62, no. 1, pp. 33–41, 2018.

[7] J. Warnatz, U. Maas, and W. R. Dibble, "Combustion: Physical and Chemical Fundamentals, Modeling and Simulation, Experiments, Pollutant Formation," *Springer-Verlag, Berlin Heidelberg, New York*, 2006.

[8] V. Bykov, I. Goldfarb, and V. M. G. B. J. Greenberg, "Auto-ignition of a polydisperse fuel spray,," *Proceedings of the Combustion Institute*, vol. 31, no. 2, pp. 2257–2264, 2007.

[9] O. Nave, V. M. Gol'dshtein, and V. Bykov, "A probabilistic model of thermal explosion in polydisperse fuel spray," *Applied Mathematics and Computation,*, vol. 217, no. 6, pp. 2698–2709, 2010.

[10] S. Sazhin, S. Martynov, T. Kristyadi, C. Crua, and M. R. Heikal, "Diesel fuel spray penetration, heating, evaporation and ignition:Modelling vs. experimentation," *International Journal of Engineering Systems Modelling and Simulation*, 2008.

[11] F. A. Williams, *The Fundamental Theory of Chemically Reacting Flow System.* Benjamin-Cummings, CA Menlo Park, 1985.

[12] V.V.Tyurenkova, "Non-equilibrium diffusion combustion of a fuel droplet," *Acta Astronautica*, vol. 75, p. 78–84, 2012.

[13] P. Rosin and E. Rammler, "Laws governing the fineness of powdered coal,." *Journal of the Institute of Fuel*, vol. 7, pp. 29–36, 1933.

[14] S. Nukiyama and Y. Tanasawa, "Experiments on the atomization of liquids in an airstream," *Transactions of the Japan Society of Mechanical Engineers*, vol. 5, pp. 68–75, 1939.